

RSC Advances



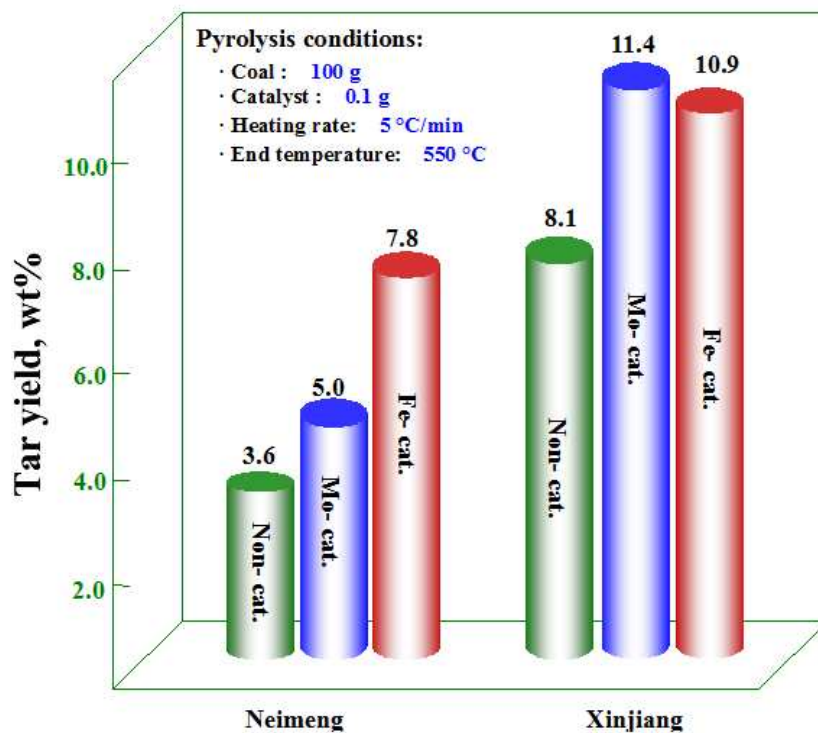
This is an *Accepted Manuscript*, which has been through the Royal Society of Chemistry peer review process and has been accepted for publication.

Accepted Manuscripts are published online shortly after acceptance, before technical editing, formatting and proof reading. Using this free service, authors can make their results available to the community, in citable form, before we publish the edited article. This *Accepted Manuscript* will be replaced by the edited, formatted and paginated article as soon as this is available.

You can find more information about *Accepted Manuscripts* in the [Information for Authors](#).

Please note that technical editing may introduce minor changes to the text and/or graphics, which may alter content. The journal's standard [Terms & Conditions](#) and the [Ethical guidelines](#) still apply. In no event shall the Royal Society of Chemistry be held responsible for any errors or omissions in this *Accepted Manuscript* or any consequences arising from the use of any information it contains.

Graphical abstract:



Textual abstract:

Catalyst dissolved in an accessory ingredient and was sprayed into coal particles, in this case, even the active catalyst content was only 0.1 wt%, a good catalytic effect could be generated for the depolymerization of coal.

Mild catalytic depolymerization of low rank coals: A novel way to increasing tar yield

Litong Liang^a, Wei Huang^{a,*}, Fuxing Gao^a, Xiaogang Hao^b, Zhonglin Zhang^b, Qian Zhang^a, Guoqing Guan^c

(^a Key Laboratory of Coal Science and Technology of Ministry of Education and Shanxi Province, Taiyuan University of Technology, Taiyuan 030024, Shanxi, China)

(^b Department of Chemical Engineering, Taiyuan University of Technology, Taiyuan 030024, Shanxi, China)

(^c North Japan Research Institute for Sustainable Energy, Hirosaki University, 2-1-3 Matsubara, Aomori 030-0813, Japan)

* Corresponding author. Tel: +86 0351 6018073; E-mail address: huangwei@tyut.edu.cn.

Abstract: Mild catalytic depolymerization of two kinds of low-rank coals named as Neimeng and Xinjiang coals sprayed with Mo- and Fe-based catalyst were performed in a batch reactor. The obtained tar was analyzed by gas chromatography/mass spectrometry (GC/MS), and the coal and char were characterized by Raman and fourier transform infrared spectroscopy (FTIR). The results indicated that the tar yields for Neimeng coal were increased from 3.6 % to 5.0 % and 7.8 % while those for Xinjiang coal were increased from 8.1 % to 11.4 % and 10.9 % after the addition of Mo- and Fe-based catalysts, respectively. Based on the GC/MS analysis, it is found that the hydroxybenzene content was significantly decreased while naphthalene contents was increased in the tar derived from Neimeng coal when Mo-based catalyst was used. In contrast, the production of light aromatics was enhanced by the addition of Fe-based catalyst. For comparison, the production of aromatics from Xinjiang coal was remarkably inhibited but the content of aliphatic hydrocarbon was significantly increased after the addition of catalyst. The Raman and FTIR analyses results indicated that the catalyst could improve the reaction of hydrogen free radicals with char, which was benefit to the depolymerization of coal.

Keywords: Low rank coals; catalytic depolymerization; tar; Mo-based catalyst; Fe-based catalyst.

1. Introduction

Increasing of fossil fuel consumption in recent years has led to an alarming concerns in the emission of greenhouse gases [1]. Thus it is urgent for controlling carbon emissions and improving energy efficiency in the world, especially in China, who consumes the largest amount of coal [2, 3]. Coal is a solid fuel in which complex organic matter is the major component and inorganic matter is the minor component [4-7]. Thermal conversion is the main way for its utilization [8]. Traditional ways such as direct combustion and gasification are generally to break all chemical bonds in coal structure and then restructure them [9]. The entire process always is arranged in a single reactor, where the various components in coal will be handled equally. This will not only destroy the high-value coal components, but also consume extra energy to break the chemical bonds causing huge energy loss and large amount of carbon emissions. In order to solve this problem, a cascade utilization of coal based on the coal structure and compositions is put forward, in which the coal is decomposed in stages by controlling temperature and pressure, and this will be the most effective way to use coal resource [10].

Pyrolysis is an effective way to produce oil and high value-added chemicals from coal and its also the first step of cascade utilization of coal [10]. To date, a variety of coal pyrolysis technologies such as Lurgi [7], LFC [8], Toscoal [8], and COED [10], have been commercially demonstrated. In China, for the desiring of upgrading oil from the large reserve of low rank coal [11], several research institutes such as in Dalian University of Technology, Zhejiang University, Taiyuan University of Technology, and Institute of Process Engineering, Chinese Academy of Sciences have also developed their unique pyrolysis technologies. However, due to the lack of fundamental researches on the complexity structure of coal and its decomposition characteristics at different conditions, no one commercial pyrolysis plant is running well until now [12, 13]. Especially, in order to improve the energy efficiency during pyrolysis, it is favorable to realize this process in a relatively low temperature. However, at mild or low temperature, pyrolysis is generally not easy to achieve high conversions. Therefore, some novel ways such as catalyst-assisted pyrolysis processes should be developed.

Inorganic compounds have been found to have significantly catalytic effect on the yield and composition of product during coal pyrolysis [14]. Nursen et al. blended metal chlorides (CoCl_2 ,

NiCl₂, ZnCl₂, CuCl₂ and Fe₂O₃·SO₄) with coal and used a thermogravimetric analyzer to investigate the effects of these chlorides [15]. The results indicated that the addition of these chlorides increased the conversion significantly. Zhu et al. blended the coal with CaO (12 wt%) first and then carried out the pyrolysis process under atmospheric pressure over a temperature range of 450-750°C in a fluidized bed reactor. They found that the tar yield decreased while the gas yield increased [16]. Takarada et al. used catalyst as bed materials for the fluidized bed pyrolysis of coal, and obtained a high yield of hydrocarbon liquid. They found that the product yields were strongly depended on the gas atmosphere, catalyst type, pyrolysis temperature and pressure [17].

Researchers also studied the catalytic pyrolysis where the coal and catalyst are arranged separately, which is always done in a two stage reactor. This technology could be divided into two ways, one is the reacting gas first come through catalyst, then the active gas goes into the coal bed and pyrolyzed, the other is the catalytic cracking of coal pyrolysis volatiles over catalysts. During these processes, the coal and catalyst does not contact directly. Liu and Jin et al. [18, 19] arranged coal and Ni/MgO catalyst layers separately in a two stage fixed bed reactor, when CH₄/CO₂ gas mixture was used as the pyrolysis gas. They found that the tar yield increased and suggested that the free radicals cracked from coal in coal pyrolysis were remarkably stabilized by the H and CH_x groups dissociated from CO₂ reforming of methane. Han et al. [20, 21] studied the catalytic upgrading of tar derived from coal over char-based catalysts, and observed that the fraction of light tar (boiling point lower than 360 °C) as well as non-condensable gas yield increased. Some researchers impregnated coal with aqueous solution of catalyst, and then evaporated the water so that the catalyst was well dispersed on the coal [22, 23]. It is found that the impregnation method enhanced the catalytic effect and promoted the coal pyrolysis conversion.

Catalysts used in pyrolysis could active the chemical bonds through the adsorption reactive molecules selectively, and start the reaction at moderate conditions [20]. If the basic bridge bonds could be broken selectively with the catalyst assistance, the valuable aromatics will be easily obtained and simultaneously, the pyrolysis temperature will be decreased, and optimum product distribution will be obtained. Based on this, a novel catalytic pyrolysis concept, i.e., coal catalytic depolymerization was proposed by our team, in which the catalyst was tried to add in the coal

structure by adding some adjunct reagents, and this is different from conventional catalytic pyrolysis where the catalyst is added on the outside surface of coal. It is expected that by this way, the coal can be converted into high value-added chemicals or liquid fuels in mild conditions so that the energy consumption could be reduced greatly. The effect of the catalyst addition on the coal depolymerization was investigated in details and the possible reasons on tar yield changes were explained.

2. Experimental Section

2.1. Samples and pretreatment

Two lignites, i.e., Neimeng (NM) and Xinjiang (XJ), were used as low-rank coal feedstock. They were air-dried, ground, and sieved to particles with a size of 2.4- 4.8 mm. The proximate and ultimate analyses are shown in Table 1. 100 g of coal were sprayed with 5 mL solution containing molybdenum salt (Mo) or ferrum salt (Fe), accessory ingredient and water in a 250 mL beaker and then mechanically blended and stayed for 30 min. The catalyst loading amount was about 0.1 wt% (elemental metal content on dry coal basis). The so-prepared samples were then dried at 115 °C for two hours and placed in a desiccator for the subsequent experiments. The procedure is shown in Fig. 1.

2.2 Depolymerization experiment

Fig. 2 presents a schematic diagram of the depolymerization process. It was carried out in the batch reactor, which was made of stainless-steel with an inner diameter of 108 mm and a height of 250 mm in total. It was heated electrically to 250 °C, and then 100 g of the sample was feed into the reactor. After nitrogen purging, the reactor was heated up to 650 °C with a rate of 5 °C/min and holding at this temperature for 15 min.

The liquid product was collected in a cold trap maintained at a temperature of about -15 °C. The liquid phase consisted of water and tar, they were separated and weighted using a standard method in which the water content was determined by the toluene azeotropic method (GB/T480-2010). After depolymerization, the char was collected and weighted. The gases were collected and the yield was calculated by difference. The depolymerization experiments showed an acceptable

standard deviation of 1.1 wt% for the char and tar yields with three replicates.

2.3. Tar fractions

Tar fractions were analyzed by a Sataram SETSYS TGA. About 10 mg of tar was placed in an alumina crucible (8 mm inner diameter and 5 mm height) and then heated to 400 °C with a heating rate of 10 °C/min in a nitrogen flow of 100 mL/ min. All TG analyses were performed repeatedly to make sure their reproducibility. The tar fractions were divided into 5 parts by temperature ranges: 110-180 °C; 180-230 °C; 230-300 °C; 300-400 °C and higher than 400 °C.

2.4. Characterization of the tar with GC/MS

The compositions of the tar were analyzed using a Hewlett-Packard 6890/5973 GC system equipped with a capillary column coated with HP-5 MS (crosslink 5% PH ME siloxane, 30 m × 0.25 mm i.d., 0.25 μm film thickness) and a quadrupole analyzer operated in electron impact (70 eV) mode. The mass range scanned was from 30 to 500 amu. The column was heated at a heating rate of 20 °C min⁻¹ from 100 to 300 °C and held at 300 °C for 10 min. Data were acquired and processed using Chemstation software. The compounds were identified by comparing mass spectra with NIST05 library data.

2.5. FTIR spectroscopy analysis

Infrared (IR) spectra of the coal and char were obtained using a FT-IR spectrometer (VERTEX70 spectrometer) using pellet technique. Prior to FTIR analysis, KBr and samples were kept in an oven at 110 °C for 2 h to remove external water. KBr pellets were prepared by grinding the mixture of 1 mg of sample with 200 mg of KBr. The spectra were recorded from 4000 to 400 cm⁻¹ at 8 cm⁻¹ resolution.

2.6. Raman spectroscopy analysis

Raman analyses of coal and char were performed by RENISHAW- in Via Ramam Microscope with laser power 20mW × 5% (1mV), laser wave length of 514.5 nm and scan range of 800~1800 cm⁻¹.

3. Results and discussion

3.1. Tar analysis

3.1.1. Tar yields

Table 2 shows tar yields from the depolymerization of both coal samples with and without catalyst at 650 °C. Compared with the case without catalyst, the tar yield increased significantly with the catalyst addition. The tar yield from NM coal with Mo-based catalyst was 5.0%, which was higher than that of without catalyst (tar yield was 3.6%), and was a little lower than that of with Fe-based catalyst (tar yield was 7.8%). In the case by using Fe-based catalyst, the tar yield from NM coal was about 2.2 times higher than that from the raw NM coal depolymerization. In contrast, for XJ coal, both Mo- and Fe-based catalysts obviously enhanced the tar yield, and the tar yields increased to 11.4% and 10.9%, respectively, which were relatively about 1.4 and 1.35 times as that of raw XJ coal depolymerization (tar yield was 8.1%).

3.1.2 Elemental analysis

Elemental analysis results (dry basis) for the tar derived from the coals with and without catalysts are shown in Table 3. For NM coal, the hydrogen content and H/C molar ratio decreased slightly in the presence of catalysts. The highest tar yield from NM coal was obtained when Fe-based catalyst added, while the hydrogen content in the tar was the lowest, indicating that the components with lower H/C molar ratios were increased with the addition of catalyst. In contrast, for the tars derived from XJ coal, the hydrogen content and H/C molar ratio increased obviously when catalyst was added, which indicated that the components with higher H/C molar ratios increased.

3.1.3 Tar fractions

The amount of tar fractions obtained from coal depolymerization with different catalysts are shown in Table 4. For NM coal with different catalysts, there were little changes in the tar fractions. Combined with the elemental analysis above, though the hydrogen content of the tar decreased when catalyst was added, the change was tiny and the heavy tar formation tendency was

not observed here. This indicated that the increase of tar yield could be related to the increase of broad molecular compounds. In contrast, for XJ coal, the tar percentages of 180-230°C and 230-300°C fractions for catalytic coal depolymerization increased obviously compared with that in the absence of catalyst. This indicated that both Mo and Fe-based catalysts not only enhanced the tar yield but also improved the quality of the tar.

3.1.4 GC/MS analysis

The total ion chromatographs (TICs) analyses of the depolymerization tar from the coals with or without catalysts are presented in Fig. 3. All detected compounds were categorized into paraffins, olefins, phenols, 1-ring, 2-ring, 3-ring aromatics and others. The chromatograms revealed that the compositions of tar from the catalytic depolymerization of the two types of coal were similar. But the contents of components of the tars varied obviously. Fig. 4 depicts the changes of various species of tar from depolymerization of coals with and without catalysts. As presented in Fig. 4, the yields of paraffins, olefins and aromatics from the catalytic depolymerized tar of NM coal increased. Especially, the 2-ring aromatics yield in the tar of Mo-based catalytic depolymerization increased a lot. The yields of phenols, 1-ring aromatics and 2-ring aromatics in the tar derived from Fe-based catalytic depolymerization also enhanced. That is, with the catalyst addition, the contents of most of the components in the tar increased, though the tar hydrogen content decreased a little, as shown in Table 3 (the H content decreased about 0.23% and 0.80%, respectively). In contrast, for the catalytic depolymerization of XJ coal, the yields of paraffins, olefins and phenols increased greatly, whereas the 2-ring aromatics yield decreased significantly. The 1-ring aromatics and 3-ring aromatics changed a little. The incremental components of the tar were mainly the aliphatics with high ratio of H/C, causing the H content in the tar increased significantly, as shown in Table 3 (the H content increased about 1.16 % and 2.28%, respectively).

Combined with Fig. 3, the incremental aliphatics from the tar derived from two coals were mainly those with long chains. This indicated that there were a certain number of alicyclic structures in coals, whose main chemical bonds were $C_{al}-C_{al}$, $C_{ar}-C_{ar}$, $C_{ar}-C_{al}$ and $C_{al}-H$, $C_{ar}-H$ (the bond energy is shown in Table 5 [24]). Breaking of these bonds is mainly related to the reaction temperature. Chemical bonds with lower energy (No. 01- 04) would be broken in the conventional

pyrolysis process without catalyst, whereas the bonds with higher energy (No. 05- 08) could be also broken and simultaneously the cycloalkane could be open in the presence of catalyst during this process. The catalysts could make the macromolecules of coal depolymerize into smaller cell structure [25]. And the aryl radicals in the char with side chains could combined with the hydrogen radicals, which decrease the combinational opportunity of aryl radicals and hydrocarbon radicals with those long chains. As a result, the hydrocarbon radicals with long chains could link with each other to form more large molecules, thus increasing the tar yield.

3.2 Char analysis

3.2.1 Yield and elemental analysis

Table 6 shows the char yield during the coal depolymerization at 650 °C with and without catalyst. The elemental analysis of the coal and char are shown in Table 7. The vast hydrogen atoms in coal are directly connected with carbon atoms. The H/C atomic ratio can basically reflect the degree of coalification. The conventional coal pyrolysis is similar to the conversion of low rank coal to high rank coal. The coal pyrolysis conversion are generally enhanced after adding catalyst and thus, the corresponding H/C atomic ratio would be reduced. However, in this study, the H/C atomic ratios for all catalytic depolymerization chars were found to be slightly increased, as shown in Table 7. This indicated that the catalyst promoted the reaction of hydrogen radicals with char fragments, and inhibited the condensation between char fragments, which will be further discussed in the following.

3.2.2 FT-IR spectroscopy

IR spectra of the coal and char are shown in Fig. 5. The degree of coal metamorphism could be reflected by aliphatic and aromatic hydrogen. Hence the IR spectra of the 3000- 2800 cm^{-1} zone for aliphatic hydrogen stretching and the 900- 700 cm^{-1} zone for aromatic hydrogen bending were curve-fitted [10, 26]. Accordingly, the absorptivity of aliphatic and aromatic hydrogen is 744 cm^{-1} and 684 cm^{-1} , respectively [27]. Combined with element analysis, the ratio of aliphatic and aromatic hydrogen and the atomic ratio of aromatic H/C were calculated. As shown in Table 8, the content of aliphatic hydrogen decreased with the catalyst addition, while the content of aromatic hydrogen and the ratio of aromatic H/C increased. This indicates that the catalyst promoted the cleavage of the $\text{C}_{\text{ar}}\text{-C}_{\text{al}}$ bonds. Once the aliphatic chains fall off from aromatic nuclei, hydrogen

free radicals will combine with these nucleus, increasing the content of aromatic hydrogen and corresponding aliphatic hydrocarbons in tar. Furthermore, the increase of hydrogen contents in char could be mainly attributed to the increasing of hydrogen content in the aromatic nuclei.

3.2.3 Raman spectroscopy

Fig. 6 shows the Raman spectra of the coal and char. According to the semi-quantitative analysis method [27, 28], the Raman spectra of coal and char could be fitted into 10 representative bands. Fig. 7 shows the spectral deconvolution of the char from the depolymerization of NM coal with Fe-based catalyst. The deconvolution of the char spectra revealed that the main bands were the G and D bands. The G band mainly represents aromatic ring vibration, the D band represents the degree of condensation for greater aromatic ring systems (no less than 6 fused aromatic rings). The other three bands G_R , V_L , V_R , assigned in the region between the G and D bands, can represent the degree of condensation for smaller aromatic ring systems (3-5 fused aromatic rings).

After curve-fitting of Raman spectra of coal and char, the ratio of peak areas for these main bands are shown in Table 9. The I_D/I_G ratio between the D band and G band intensities (peak area) is used as an important parameter to study the crystalline or graphite-like carbon structures, and the increase of I_D/I_G in char is generally related to the increase content of large aromatic rings that have six or more fused benzene rings. The ratio of I_D/I_G in char decreased slightly with the addition of catalyst, indicating that contents of large aromatic rings (≥ 6 rings) decreased. This also indicates that the addition of catalyst reduce the condensation reactions, which is benefit for the further depolymerization of coal. The G_R , V_L , V_R bands between the G and D bands represent the typical structures in an amorphous carbon. They represent the smaller aromatic rings (3-5 rings). The $I_D/I_{(G+V_L+V_R)}$ ratio between the D and the combined $G+V_L+V_R$ peak areas can be considered as a rough measurement of the ratio between the large aromatic rings (≥ 6 rings) and the small aromatic rings (3-5 rings) in amorphous carbon [17, 18]. Table 9 shows $I_D/I_{(G+V_L+V_R)}$ decreases with adding of catalyst, revealing that the content of the smaller aromatic rings (3-5 rings) increases. This result is consistent with the FT-IR analysis where the concentration of aliphatic hydrogen and the atomic ratio of aromatic H/C increased. The existance of catalyst facilitates the incorporation of hydrogen radicals and char fragments, prohibiting the enlargement

of aromatic rings caused by the condensation of char fragments.

3.3 Carbon and hydrogen distribution in the products

Figs. 8-10 show the hydrogen, carbon distribution and the H/C ratio after depolymerization of coal with and without catalyst. When the catalyst was added, the hydrogen or carbon content in the tar increased for both coals, while for the yields of gases or chars, the change of the hydrogen or carbon content was different. This reflected that different catalysts could result in different depolymerization reaction routes.

For the catalytic depolymerization of NM coal with Mo-based catalyst, the carbon content in the char increased. During the catalytic depolymerization, the Mo-based catalyst could destroy the cage effect of the hydrogen free radical fragments, which will provide the chance for hydrogen to react with the tar precursors. In addition, Mo could inhibit the oxygen reacting with hydrogen, which will decrease the yield of water and the phenol content in tar, and increase the CO and CO₂ contents. For the catalytic depolymerization of NM coal with Fe-based catalyst, the content of carbon in the char decreased while that of the hydrogen increased. This reflected that the catalyst could increase the breakdown of the chemical bonds, and more small groups would depolymerized from the macromolecule structures. Furthermore, the Fe-based catalyst could also destroy the cage effect described above and finally increase the tar yield.

The Mo- and Fe-based catalysts showed similar effect on the depolymerization of XJ coal (Figs. 8-10), in which the carbon content in the char decreased. This indicated that the Mo and Fe catalysts could increase the breakdown of the chemical bonds, and stabilize the hydrogen free radical fragments, and finally increase the tar yield. And this is similar as the Fe-based catalyst performed for the NM coal.

It should be noted that the depolymerization of the coal in this study was done under no hydrogen atmosphere while the char and tar precursor could be stabilized by the hydrogen free radical fragments. Thus the increase of the tar yield during catalytic depolymerization could be attributed to the effect of the catalyst, which not only made the coal decomposed into more small structures or char fragments, but also increase the chance of the hydrogen free radical fragments reacting with hydrocarbon radicals with long chains effectively.

3.4 Possible reasons on tar yield increases

During conventional catalytic pyrolysis process, coal and catalyst are solid particles and mechanically blended, as shown in Fig. 11 (a), no matter how fine the coal and catalyst are grounded, they still touched with each other on the solid-solid interface. Thus, the catalytic effect could only happen on the interface of the two solids, and limiting the total catalytic activity. In this case, as shown in Fig. 12 (a), some of the volatiles would contact with the catalyst and lead to the secondary cracking, producing more gases [15].

While in this study, the catalyst dissolved in an accessory ingredient and was sprayed into the coal particles, as shown in Fig. 11 (b), the catalyst could penetrate into the coal structure in a short time. By this way, the catalyst could be dispersed well in the coal structure and thus, even less catalyst exists (the active catalyst content was only 0.1 wt%), a good catalytic effect could be generated for the depolymerization of coal. As shown in Fig. 12(b), in this case, the catalyst could cleave the bonds in the coal structure and promote the free radicals combined with the fragments and generate more tar.

4. Conclusions

1) The tar yield via the depolymerization of the NM and XJ coals increased by the addition of the Mo- and Fe-based catalysts. Compared with the depolymerization results for raw NM coal, the tar yields were increased about 1.4, 2.2 times when the Mo- and Fe-based catalysts were added, respectively. In contrast, for XJ coal, the tar yields were increased about 1.4, 1.35 times when the Mo- and Fe-based catalysts were added, respectively.

2) For the tar produced from the catalytic depolymerization of the NM coal with Mo- and Fe-based catalysts, the increased amounts of aliphatics and aromatics were similar, and the ratio of H/C of the tar also varied not so clearly. In contrast, for the tar produced from the catalytic depolymerization of XJ coal with the Mo and Fe-based catalysts, the aromatics yields decreased greatly while the aliphatics yields and the ratio of H/C increased significantly, which could be beneficial for the further hydrotreatment.

3) The addition of the catalyst increased the depolymerization degree of the low rank coal. The concentration of aromatic nucleus of the chars decreased and with the catalyst addition. And with the broken of the aliphatics with long chains, more smaller fragments were formed so that the hydrogen free radical fragments could be used more efficiently, resulting the yields of char and tar

and the quality of tar changed clearly.

Acknowledgements

This research is financially supported by an international cooperation between China and Japan, “Technology development and process integration for high-efficiency utilization of low-rank coals based on mild depolymerization and exergy recuperation” (2013DFG60060). We are also grateful to China University of Mining & Technology for providing help on coal tar analysis.

References

- [1] Irfan MF, Usman MR, Kusakabe K. Coal Gasification in CO₂ Atmosphere and Its Kinetics since 1948: A Brief Review. *Energy*. 2011;36:12-40.
- [2] Meng F, Yu J, Tahmasebi A, Han Y. Pyrolysis and Combustion Behavior of Coal Gangue in O₂/CO₂ and O₂/N₂ Mixtures Using Thermogravimetric Analysis and a Drop Tube Furnace. *Energy Fuels*. 2013;27:2923-32.
- [3] Higman C, Tam S. Advances in Coal Gasification, Hydrogenation, and Gas Treating for the Production of Chemicals and Fuels. *Chemical Reviews*. 2013;114:1673-708.
- [4] Shi L, Liu Q, Guo X, Wu W, Liu Z. Pyrolysis Behavior and Bonding Information of Coal-A TGA Study. *Fuel Processing Technology*. 2013;108:125-32.
- [5] Saxena SC. Devolatilization and Combustion Characteristics of Coal Particles. *Progress in Energy and Combustion Science*. 1990;16:55-94.
- [6] Van Heek KH. Progress of Coal Science in the 20th Century. *Fuel*. 2000;79:1-26.
- [7] Solomon PR, Serio MA, Suuberg EM. Coal Pyrolysis: Experiments, Kinetic Rates and Mechanisms. *Progress in Energy and Combustion Science*. 1992;18:133-220.
- [8] Lu K-M, Lee W-J, Chen W-H, Lin T-C. Thermogravimetric Analysis and Kinetics of Co-Pyrolysis of Raw/Torrefied Wood and Coal Blends. *Applied Energy*. 2013;105:57-65.
- [9] Siefert N, Shekhawat D, Litster S, Berry D. Molten Catalytic Coal Gasification with in Situ Carbon and Sulphur Capture. *Energ Environ Sci*. 2012;5:8660-72.
- [10] Meng F, Yu J, Tahmasebi A, Han Y, Zhao H, Lucas J, et al. Characteristics of Chars from Low-Temperature Pyrolysis of Lignite. *Energy Fuels*. 2013;28:275-84.
- [11] Kong L, Li G, Jin L, Hu H. Pyrolysis Behaviors of Two Coal-Related Model Compounds on a Fixed-Bed Reactor. *Fuel Processing Technology*. 2015;129:113-9.

- [12] Zhou Q, Zou T, Zhong M, Zhang Y, Wu R, Gao S, et al. Lignite Upgrading by Multi-Stage Fluidized Bed Pyrolysis. *Fuel Processing Technology*. 2013;116:35-43.
- [13] Chen X, Zheng D, Guo J, Liu J, Ji P. Energy Analysis for Low-Rank Coal Based Process System to Co-Produce Semicoke, Syngas and Light Oil. *Energy*. 2013;52:279-88.
- [14] Zou X, Yao J, Yang X, Song W, Lin W. Catalytic Effects of Metal Chlorides on the Pyrolysis of Lignite. *Energy Fuels*. 2007;21:619-24.
- [15] Altuntaş Öztaş N, Yürüm Y. Effect of Catalysts on the Pyrolysis of Turkish Zonguldak Bituminous Coal. *Energy Fuels*. 2000;14:820-7.
- [16] Tingyu Z, Shouyu Z, Jiejie H, Yang W. Effect of Calcium Oxide on Pyrolysis of Coal in a Fluidized Bed. *Fuel Processing Technology*. 2000;64:271-84.
- [17] Takarada T, Onoyama Y, Takayama K, Sakashita T. Hydrolysis of Coal in a Pressurized Powder-Particle Fluidized Bed Using Several Catalysts. *Catalysis Today*. 1997;39:127-36.
- [18] Liu J, Hu H, Jin L, Wang P, Zhu S. Integrated Coal Pyrolysis with CO₂ Reforming of Methane over Ni/MgO Catalyst for Improving Tar Yield. *Fuel Processing Technology*. 2010;91:419-23.
- [19] Jin L, Zhou X, He X, Hu H. Integrated Coal Pyrolysis with Methane Aromatization over Mo/HZSM-5 for Improving Tar Yield. *Fuel*. 2013;114:187-90.
- [20] Han J, Liu X, Yue J, Xi B, Gao S, Xu G. Catalytic Upgrading of in Situ Coal Pyrolysis Tar over Ni-Char Catalyst with Different Additives. *Energy Fuels*. 2014;28:4934-41.
- [21] Han J, Wang X, Yue J, Gao S, Xu G. Catalytic Upgrading of Coal Pyrolysis Tar over Char-Based Catalysts. *Fuel Processing Technology*. 2014;122:98-106.
- [22] Quyn DM, Wu H, Hayashi J-i, Li C-Z. Volatilisation and Catalytic Effects of Alkali and Alkaline Earth Metallic Species During the Pyrolysis and Gasification of Victorian Brown Coal. Part IV. Catalytic Effects of NaCl and Ion-Exchangeable Na in Coal on Char Reactivity. *Fuel*. 2003;82:587-93.
- [23] Wu Z, Sugimoto Y, Kawashima H. Effect of Demineralization and Catalyst Addition on N₂ Formation During Coal Pyrolysis and on Char Gasification. *Fuel*. 2003;82:2057-64.
- [24] Lei S. Study on the Cleavage of Covalent Bonds in Coal Pyrolysis in Consecutive Temperature Ranges. Beijing, China: Beijing University of Chemical Technology; 2014.
- [25] Suzuki T. Development of Highly Dispersed Coal Liquefaction Catalysts. *Energy Fuels*. 1994;8:341-7.
- [26] Zhang Y, Kang X, Tan J, Frost RL. Influence of Calcination and Acidification on Structural

Characterization of Anyang Anthracites. *Energy Fuels*. 2013;27:7191-7.

[27] Li X, Hayashi J-i, Li C-Z. FT-Raman Spectroscopic Study of the Evolution of Char Structure During the Pyrolysis of a Victorian Brown Coal. *Fuel*. 2006;85:1700-7.

[28] Keown DM, Li X, Hayashi J-i, Li C-Z. Characterization of the Structural Features of Char from the Pyrolysis of Cane Trash Using Fourier Transform-Raman Spectroscopy. *Energy Fuels*. 2007;21:1816-21.

Table Captions

Table 1 Proximate and ultimate analyses of coal samples.

Table 2 Tar yields of coal depolymerization with different catalyst.

Table 3 Elemental analysis of the tar.

Table 4 The amount of different temperature fractions of tar with different catalyst.

Table 5 Chemical bond energy in coal [24].

Table 6 Char yield of coal depolymerization with different catalyst.

Table 7 Elemental analysis of coal and char.

Table 8 Structural parameters deduced from FT-IR measurements.

Table 9 The peak area ratios of some of the major bands for the different samples.

Table 1 Proximate and ultimate analyses of coal samples.

Sample	Proximate analyses (wt.%)			Ultimate analysis (wt.%)				
	M _{ad}	A _d	V _{daf}	C _d	H _d	N _d	S _d	O _d *
Neimeng	10.32	13.26	43.60	52.28	6.26	0.53	0.86	26.81
Xinjiang	1.42	5.05	34.06	78.47	4.67	0.76	0.31	10.73

*, by difference.

Table 2 Tar yields of coal depolymerization with different catalyst.

Sample	Tar yield (wt%, drying)		
	Non- cat.	Mo- cat.	Fe- cat.
Neimeng	3.6	5.0	7.8
Xinjiang	8.1	11.4	10.9

Table 3 Elemental analysis of the tar.

Sample		H _d	C _d	N _d	O _d	H /C molar ratio
		%	%	%	%	
Neimeng	Non- cat.	10.12	79.75	0.77	8.58	1.523
	Mo- cat.	9.89	80.30	0.65	8.60	1.478
	Fe- cat.	9.32	76.22	1.38	11.80	1.467
Xinjiang	Non- cat.	8.14	76.42	1.10	13.86	1.278
	Mo- cat.	10.42	82.12	0.96	6.30	1.522
	Fe- cat.	9.30	79.19	1.25	10.04	1.409

Table 4 The amount of different temperature fractions of tar with different catalyst.

Sample		<180°C	180-230°C	230-300°C	300-400°C	>400°C
		%	%	%	%	%
Neimeng	Non-cat.	10.05	24.11	30.98	22.12	12.74
	Mo- cat.	10.59	22.59	29.84	23.64	13.34
	Fe- cat.	11.32	24.33	32.89	20.43	11.03
Xinjiang	Non-cat.	12.57	25.69	29.82	19.28	12.64
	Mo- cat.	13.49	29.92	39.37	13.63	3.69
	Fe- cat.	13.05	28.47	35.71	17.65	5.12

Table 5 Chemical bond energy in coal [24].

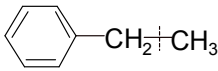
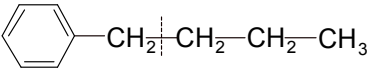
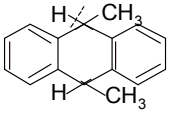
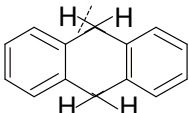
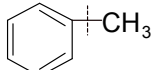
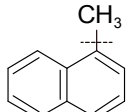
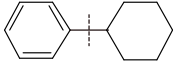
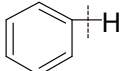
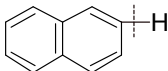
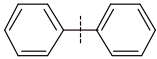
No.	Compounds	Bond types	Bond Energy (kJ/mol)
01		C _{al} -C _{al}	317.1
02		C _{al} -C _{al}	315.1
03		C _{al} -H	322.2
04		C _{al} -H	326.4
05	CH ₃ -CH ₂ -H	C _{al} -H	410.0
06		C _{ar} -C _{al}	426.8
07		C _{ar} -C _{al}	434.3
08		C _{ar} -C _{al}	413.0
09		C _{ar} -H	464.4
10		C _{ar} -H	468.2
11		C _{ar} -C _{ar}	478.6

Table 6 Char yield of coal depolymerization with different catalyst.

Sample	Char yield (wt %, dry basis)		
	Non- catalyst	Mo- catalyst	Fe- catalyst
Neimeng	69.4	70.6	65.5
Xinjiang	79.8	74.6	76.2

Table 7. Elemental analysis of coal and char.

Sample		H _d	C _d	N _d	O _d	H/C molar ratio	
Neimeng	Coal	6.26	52.28	0.53	30.8	1.44	
	Char	Non- cat.	2.61	72.52	1.06	9.01	0.43
		Mo- cat.	2.67	72.94	1.1	8.08	0.44
		Fe- cat.	2.91	76.16	1.23	7.29	0.46
Xinjiang	Coal	4.67	78.47	0.76	10.73	0.71	
	Char	Non- cat.	2.77	86.98	1.15	5.92	0.38
		Mo- cat.	2.79	87.19	1.07	4.58	0.39
		Fe- cat.	2.91	86.24	1.08	5.73	0.40

Table 8 Structural parameters deduced from FT-IR measurements.

Sample		H_{ar}/H_{al}	H_{al} (wt%)	H_{ar} (wt%)	C_{al} (wt%)	C_{ar} (wt%)	H_{ar}/C_{ar} (atomic ratio)
Neimeng	Non- cat.	1.01	1.30	1.31	8.64	63.88	0.247
	Mo- cat.	1.96	0.90	1.77	6.00	66.94	0.317
	Fe- cat.	3.43	0.66	2.25	4.38	71.78	0.377
Xinjiang	Non- cat.	0.67	1.66	1.11	11.07	75.91	0.175
	Mo- cat.	1.47	1.13	1.66	7.54	79.65	0.250
	Fe- cat.	1.62	1.11	1.80	7.41	78.83	0.274

Table 9 The peak area ratios of some of the major bands for the different samples.

Sample		I_D/I_G	$I_D/I_{(G+V1+V2)}$	
Neimeng	Coal	1.09	1.05	
	Char	Non- cat.	1.32	1.65
		Mo- cat.	1.29	1.58
		Fe- cat.	1.30	1.50
Xinjiang	Coal	1.08	1.73	
	Char	Non- cat.	1.27	2.00
		Mo- cat.	1.27	1.92
		Fe- cat.	1.24	1.94

Figure Captions

Fig. 1. Flow chart for catalyst loading.

Fig. 2. Diagram of the depolymerization reactor.

Fig. 3. GC-MS chromatograms of the primary tar.

Fig. 4. The changes of various species from depolymerization tar of coal with and without catalyst.

Fig. 5. FTIR spectra of the coal and char.

Fig. 6. Raman spectra of the coal and char.

Fig. 7. Curve fitting of a Raman spectrum of the Neimeng coal with Fe-based catalyst, the main total area ratios of the peaks are listed in Table 9.

Fig. 8. The distribution of element H in products.

Fig. 9. The distribution of element C in products.

Fig. 10. H/C atomic ratio in products.

Fig.11. The patterns of catalyst contacting with the coal.

Fig.12. The route of the coal depolymerization into coal tar.

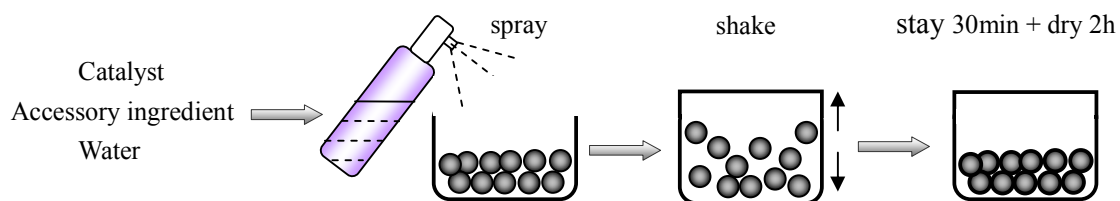


Fig. 1. Flow chart for catalyst loading.

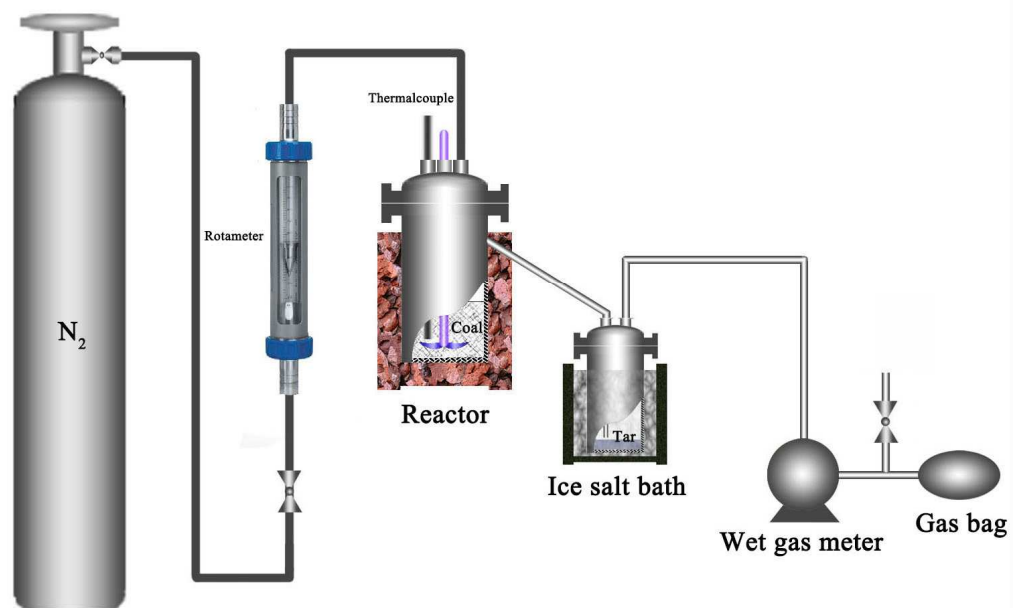
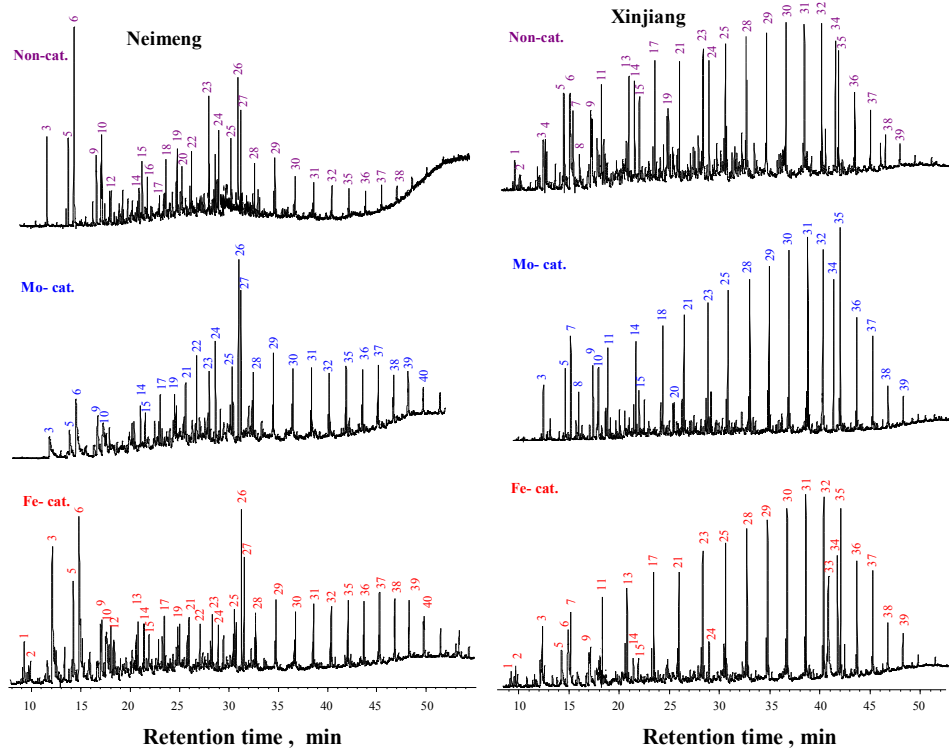


Fig. 2. Diagram of the depolymerization reactor.



Peak Number	Compound	Peak Number	Compound
1	p-Xylene	21	C15
2	C9	22	Naphthalene, 1,2,3,4-tetrahydro-5,6,7,8-tetramethyl-
3	Phenol	23	C16
4	C10	24	Naphthalene, 2,3,6-trimethyl-
5	Phenol, 2-methyl-	25	C17
6	Phenol, 4-methyl-	26	1-Dodecanol, 3,7,11-trimethyl-
7	C11	27	9H-Fluorene, 9-methyl
8	Benzofuran, 2-methyl-	28	C18
9	Phenol, 2,6-dimethyl-	29	C19
10	Phenol, 4-ethyl-	30	C20
11	C12	31	C21
12	Naphthalene	32	C22
13	C13	33	Phenanthrene, 2,3,5-trimethyl-
14	Naphthalene, 2-methyl-	34	Phenanthrene, 1-methyl-7-(1-methylethyl)-
15	Naphthalene, 1-methyl-	35	C23
16	2,5,6-Trimethylbenzimidazole	36	C24
17	C14	37	C25
18	Naphthalene,2,6-dimethyl-	38	C26
19	Naphthalene, 2,7-dimethyl-	39	C27
20	Hexadecane, 7,9-dimethyl-	40	C28

Fig. 3. GC-MS chromatograms of the primary tar.

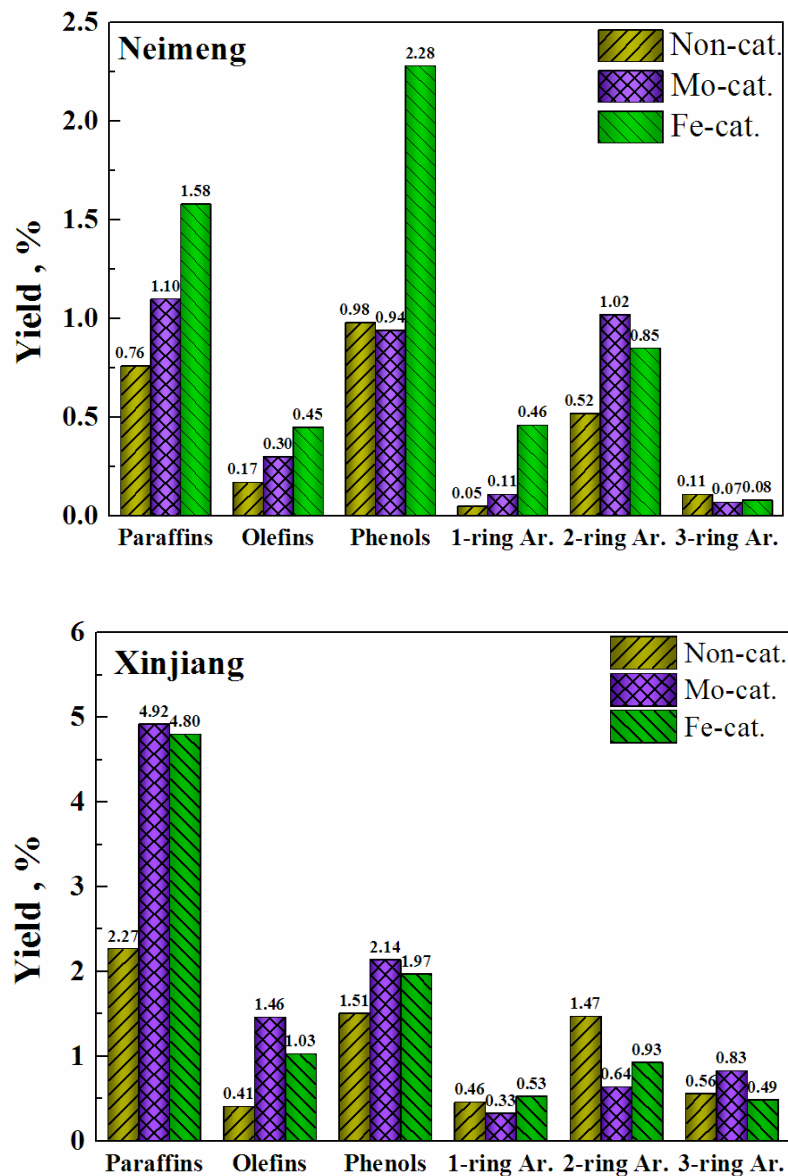


Fig. 4. The changes of various species from depolymerization tar of coal with and without catalyst.

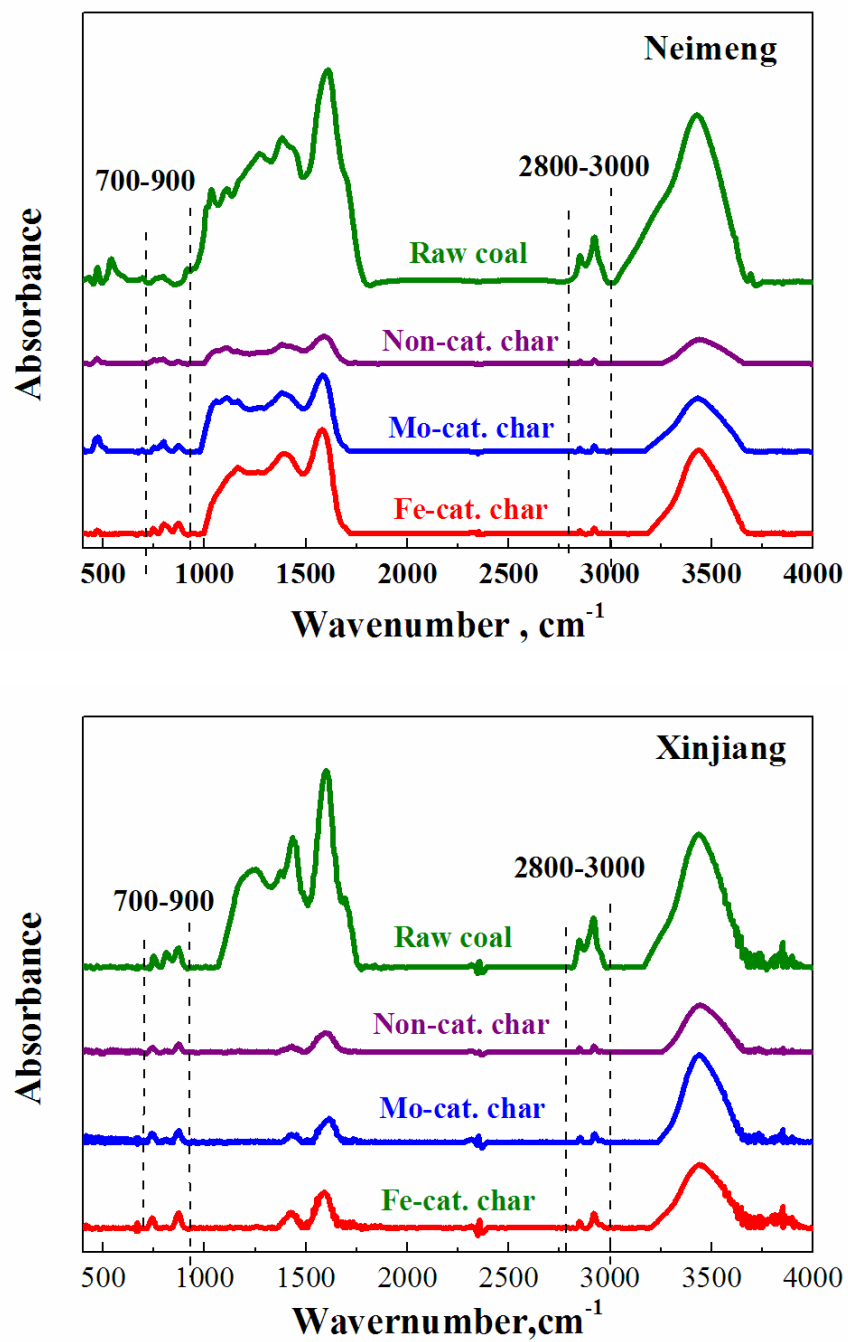


Fig. 5. FTIR spectra of the coal and char.

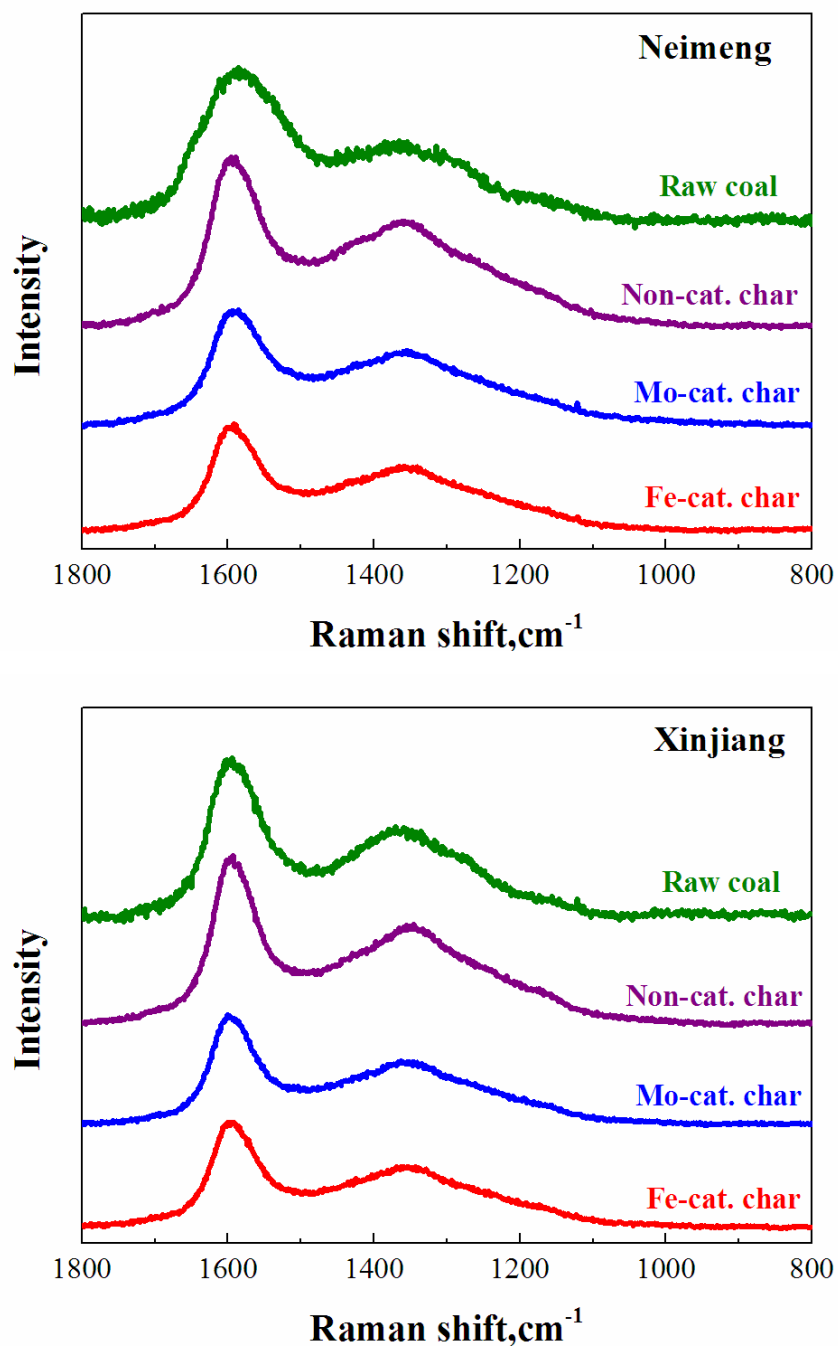


Fig. 6. Raman spectra of the coal and char.

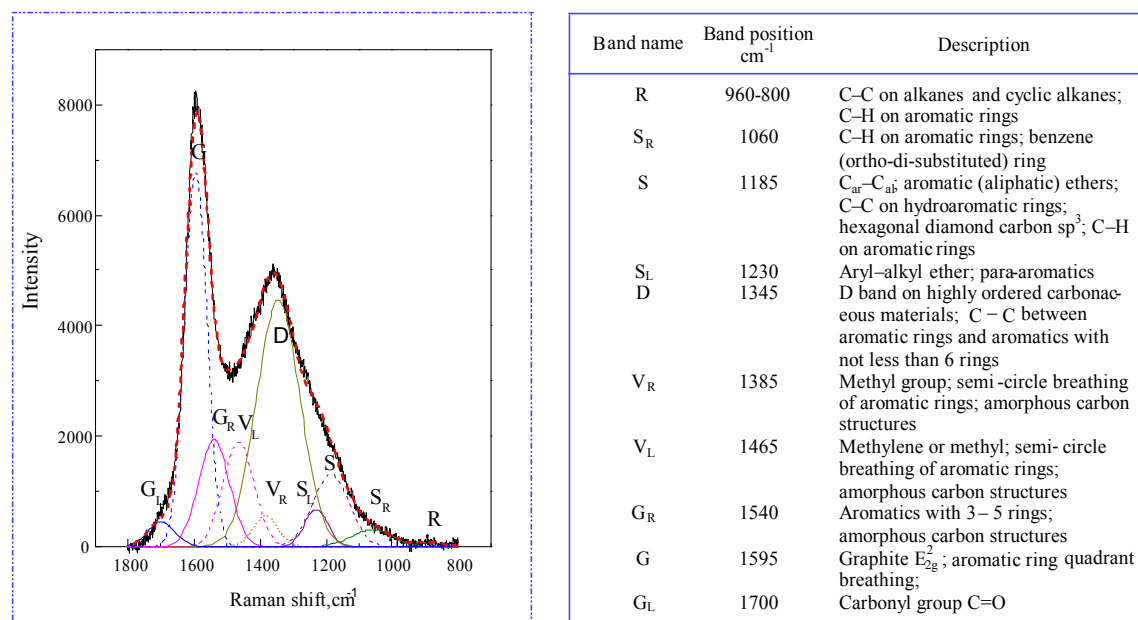


Fig. 7. Curve fitting of a Raman spectrum of the Neimeng coal with Fe-based catalyst, the main total area ratios of the peaks are listed in Table 9.

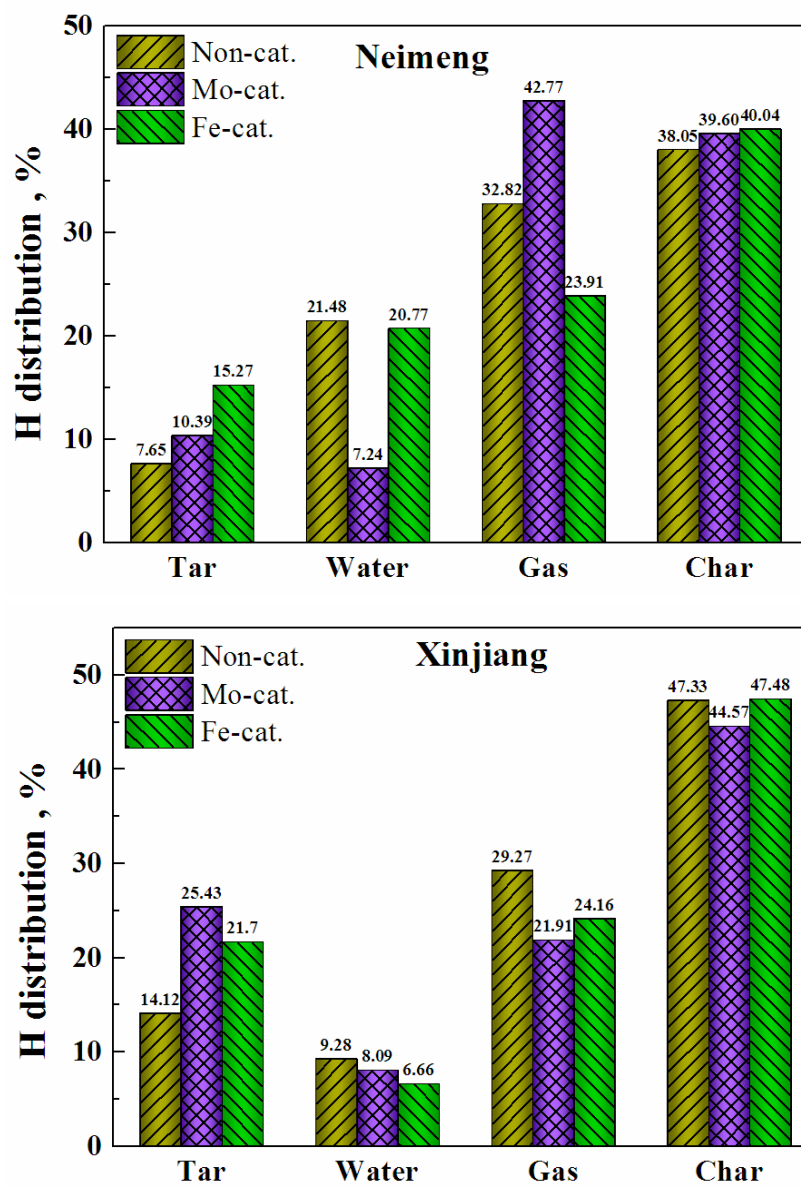


Fig. 8. The distribution of element H in products.

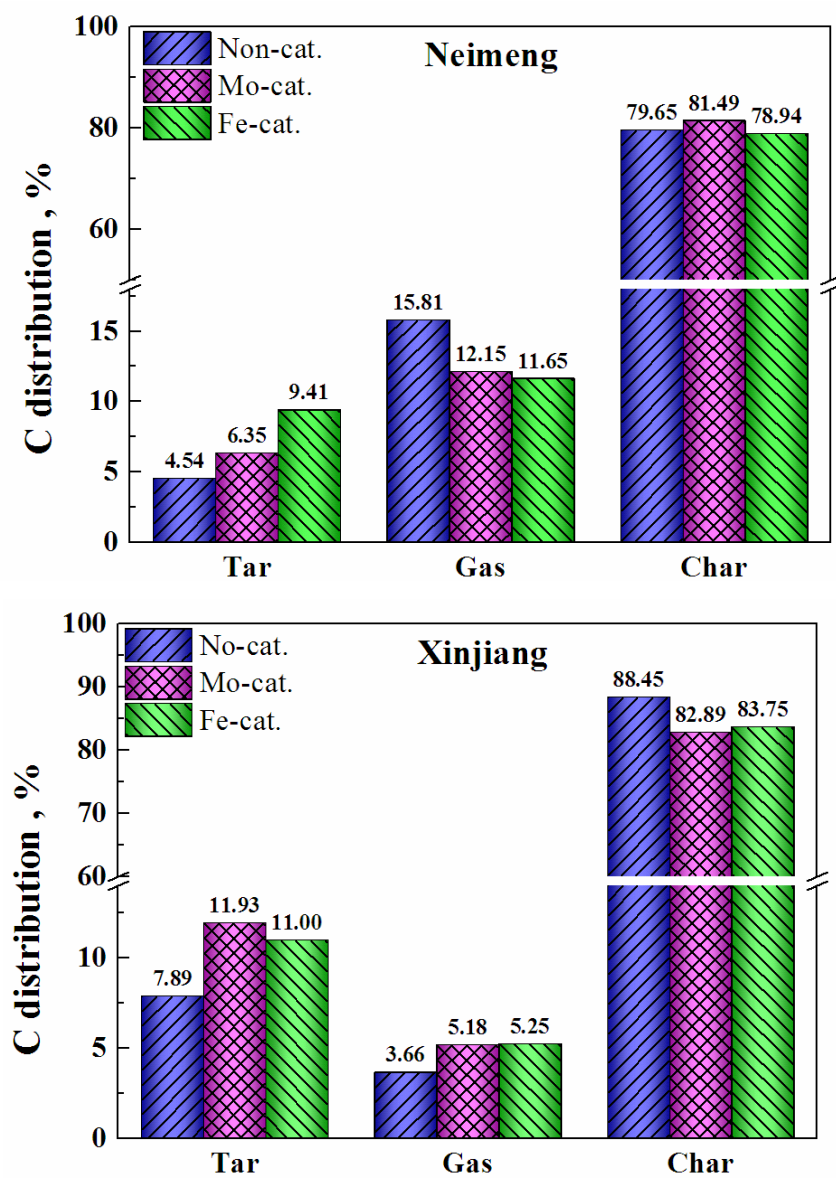


Fig. 9. The distribution of element C in products.

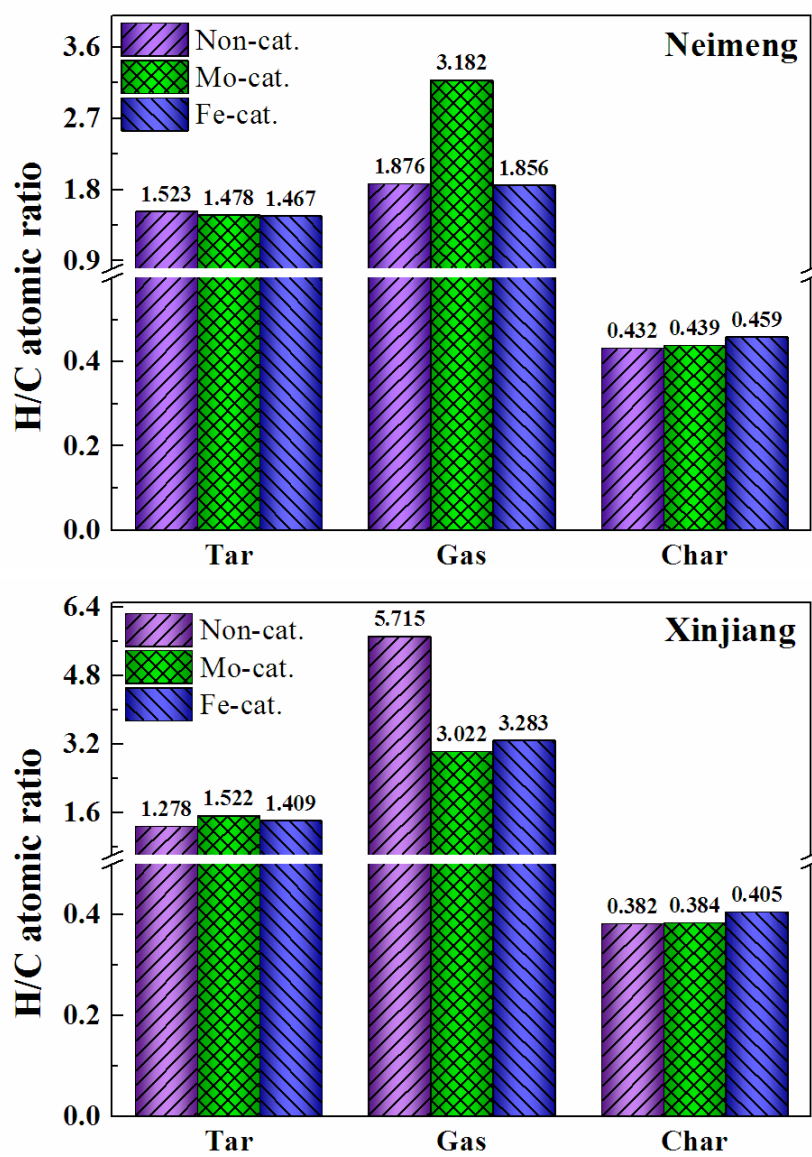


Fig. 10. H/C atomic ratio in products.



Fig.11. The patterns of catalyst contacting with the coal.

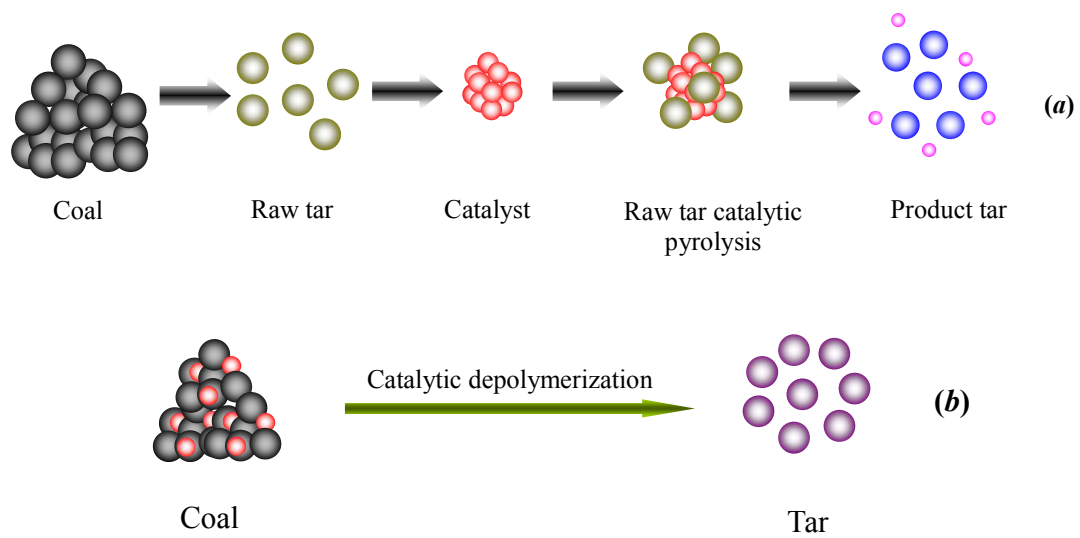


Fig.12. The route of the coal depolymerization into coal tar.